UNSTEADY RADIATIVE FLOW, HEAT AND MASS TRANSFER THROUGH A SQUEEZING CHANNEL IN THE PRESENCE OF JOULE HEATING AND HEAT SOURCE/SINK

By
Suresh Kumar
Govt. College, Bidasar, Churu-331501, Rajasthan, India
Email id: smusumaths@gmail.com

Sushila Choudhary
Department of Mathematics, University of Rajasthan, Jaipur-302004, India
Email id: sumathru11@gmail.com

Anil Sharma
Department of Mathematics, University of Rajasthan, Jaipur-302004, India
Email id: anilsharma9414@gmail.com

Abstract
Unsteady MHD flow, heat and mass transfer of an incompressible electrically conducting viscous fluid squeezed between two infinite non conducting parallel plates separated by variable distance in the presence of heat source/sink and Joule heating effect is investigated. Radiation and dissipation effects also considered here. The momentum, energy and concentration equations governing the MHD squeeze flow are reduced to non linear ordinary differential equations by using similarity transformations. Approximate solution of equations subject to the appropriate boundary conditions is obtained by using fourth order Runge-Kutta method with shooting technique. The effects of different physical parameters on velocity, temperature and concentration distributions are discussed through graphs. The skin friction coefficient, Nusselt number and Sherwood number are derived, discussed numerically and their numerical values for various values of physical parameters are presented through tables.

Key words: MHD, Squeeze flow, Radiation, Heat source/sink, Joule heating.
DOINumber: 10.48047/NQ.2022.20.20.NQ109055 **NeuroQuantology2022;20(20): 523-534**

1. INTRODUCTION

Squeezing flow has broad applications in many fields such as bio-mechanics, food industries, chemical and mechanical engineering. In squeeze flow, material is compressed between two parallel plates by applying a constant velocity or normal stresses by means of a mobile boundary. This process is frequently analyzed in hydro-dynamical machines, electric motors, engines, hydraulic lifters etc. Practically, squeezing flow is used in polymer processing, compression and injection molding, modeling of hydrodynamic lubrication system etc. The use of a MHD fluid in lubrication prevents the adverse impact of temperature on the fluid viscosity when the system operates under extreme conditions. In heat pumping technology natural heat source/sinks like air, ground, water etc. are used. This technology plays a significant role in

eISSN 1303-5150

manufacture of compressors, refrigerators and air conditioners. The study of heat transfer is necessary for safe and consistent working of rapidly moving engines and machines with lubricants inside. Therefore, study of heat transfer in such type of system has become an active field of research.

Stefan (1874) was the first who presented basic formulation of squeezing flows under lubrication assumption. A study of squeezing flow has been done by Jackson (1962). Wang (1976) discussed the squeezing of fluid between two plates. The magnetohydrodynamic squeeze film has been considered by Hamza (1988). Makinde *et al.* (2002) presented the bifurcation analysis in nonlinear squeezing flow between two parallel plates. A study on heat transfer effects in a viscous fluid squeezed and extruded between two parallel plates has been shown by Duwairi (2004). Mahmood *et al.* (2007) analyzed the squeezed flow and heat transfer over a porous surface for viscous fluid. Unsteady squeezing flow of a viscous MHD fluid between parallel plates has been solved by Siddiqui *et al.* (2008) using the homotopy perturbation method. Influence of heat transfer in the squeezing flow between parallel disks has been observed by Hayat *et al.* (2012). Mustafa *et al.* (2012) studied heat and mass transfer in the unsteady squeezing flow between parallel plates. MHD flow of an incompressible fluid through porous medium between dilating and squeezing permeable walls has been analyzed by Ahmed *et al.* (2014). Khan *et al.* (2014) studied unsteady two-dimensional and axisymmetric squeezing flow between parallel plates. Unsteady squeezing flow of Casson fluid between parallel plates has been considered by Khan *et al.* (2014). Ahmed *et al.* (2015) investigated the effects of magnetic field in squeezing flow of a Casson fluid between parallel plates. Sobamowo and Akinshilo (2018) has been analyzed nanofluid flow squeezed between two parallel plates under the influence of magnetic field. Unsteady Casson nanofluid squeezing flow between two parallel plates embedded in a porous medium under the influence of magnetic field is examined by Sobamowo *et al.* (2019). Jyothi *et al.* (2021) studied the Casson hybrid nanofluid flow squeezed between parallel plates with a heat source or sink and thermophoretic particle deposition. Qayyum and Oscar (2021) explored the unsteady squeezing flow through Least Squares Homotopy Perturbation Method.

The aim of paper is to investigate MHD radiative flow, heat and mass transfer of an incompressible electrically conducting viscous dissipative fluid squeezed between two parallel infinite plates separated by variable distance $h(t)$ at time t, in the presence of heat source/sink and joule effects. The effects of different physical parameters on velocity, temperature and concentration distributions are shown through graphs. Also, the effects of physical parameters on skin friction coefficient, Nusselt number and Sherwood number at the plates are also discussed numerically and their numerical values are presented through tables.

2. MATHEMATICAL FORMULATION

The unsteady MHD flow, heat and mass transfer of an incompressible electrically conducting viscous fluid squeezed between two infinite non conducting parallel plates separated by variable distance $h(t) = d\sqrt{1-at}$ at any time t, where d is the initial distance between the

eISSN 1303-5150

plates (at time $t=0$) is considered. Here $a>0$ corresponds to the movement of upper plate towards the lower static plate until they touch each other at $t=1/a$, while $a<0$ stands for its movement far away from the lower plate. Porous medium between the plates is considered. The x-axis is taken along the lower plate and y-axis is taken perpendicular to the plates. The flow is generated by the motion of upper plate at $y=h(t)$ with velocity $v_w=\frac{-da(1-at)^{-1/2}}{2}$ towards the static lower plate at $y=0$. A non-uniform magnetic field $B^*=B_0(1-at)^{-1/2}$ is applied perpendicular to the plates, where B_0 is the constant magnetic field intensity. The magnetic Reynolds is taken to be small and therefore the induced magnetic field is neglected. There is no externally applied electric field. Viscous dissipation, radiation and joule effects are also considered. T_s and T_m are the constant temperatures of the lower and upper plates, respectively. A non-uniform heat source/sink is also applied. All the fluid properties are assumed to be constant throughout the motion. This formulation has limitation as time can be varied from 0 to $1/a$, in the cases when $t>1/a$ this model cannot be used.

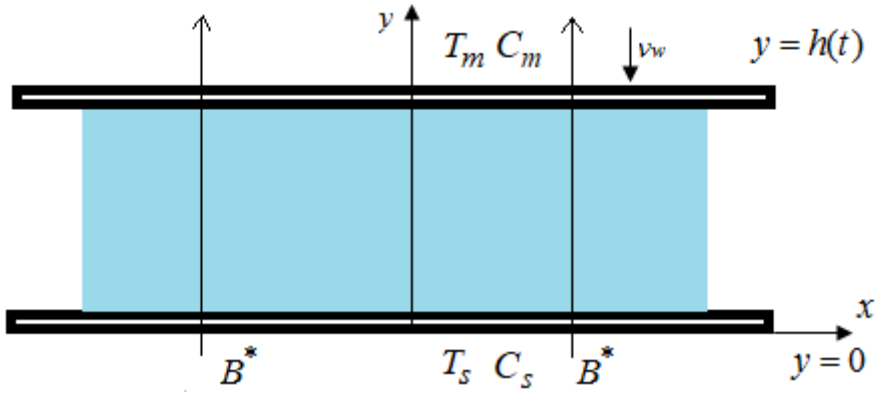

Fig.1. Physical model and the coordinate system.

Under these assumptions, the governing boundary layer equations are as follows:

Equation of continuity

$$\frac{\partial u}{\partial x}+\frac{\partial v}{\partial y}=0, \qquad (1)$$

Equation of motion

$$\rho\left(\frac{\partial u}{\partial t}+u\frac{\partial u}{\partial x}+v\frac{\partial u}{\partial y}\right)=-\frac{\partial p}{\partial x}+\mu\left(\frac{\partial^2 u}{\partial x^2}+\frac{\partial^2 u}{\partial y^2}\right)-\sigma_e B^{*2}u-\frac{\mu}{K^*}u, \qquad (2)$$

$$\rho\left(\frac{\partial v}{\partial t}+u\frac{\partial v}{\partial x}+v\frac{\partial v}{\partial y}\right)=-\frac{\partial p}{\partial y}+\mu\left(\frac{\partial^2 v}{\partial x^2}+\frac{\partial^2 v}{\partial y^2}\right)-\frac{\mu}{K^*}v, \qquad (3)$$

where u and v are fluid velocity components along x and y- directions, respectively, ρ is the density of the fluid, p is the pressure, μ is the coefficient of viscosity, σ_e is the electric conductivity, B^* is the non-uniform magnetic field and $K^*=K_0(1-at)^{1/2}$ is the porosity of the medium.

Now, introducing the vorticity function (ω) and generalized pressure (P) as

eISSN 1303-5150

$$\omega = \frac{\partial v}{\partial x} - \frac{\partial u}{\partial y} \text{ and } P = \frac{\rho}{2}\left(u^2 + v^2\right) + p \quad (4)$$

and eliminating the pressure terms from equations (2) and (3), we get

$$\frac{\partial \omega}{\partial t} + u\frac{\partial \omega}{\partial x} + v\frac{\partial \omega}{\partial y} = \nu\left(\frac{\partial^2 \omega}{\partial x^2} + \frac{\partial^2 \omega}{\partial y^2}\right) - \left(\frac{\sigma_e B^{*2}}{\rho} + \frac{\nu}{K^*}\right)\frac{\partial u}{\partial y} \quad (5)$$

Equation of energy

$$\rho C_p\left(\frac{\partial T}{\partial t} + u\frac{\partial T}{\partial x} + v\frac{\partial T}{\partial y}\right) = \kappa\frac{\partial^2 T}{\partial y^2} - \frac{\partial q_r}{\partial y} + \mu\left(\frac{\partial u}{\partial y}\right)^2 + \sigma_e B^{*2}u^2 + Q^*\left(T - T_s\right), \quad (6)$$

where T is the fluid temperature within the boundary layer, C_p is the specific heat at constant pressure, κ is the thermal conductivity, q_r is the radiative heat flux and $Q^* = Q_0\left(1-at\right)^{-1}$ is the non-uniform heat source/sink, where Q_0 is a constant initial heat source/sink.

The radiative heat flux is defined as follows

$$q_r = -\frac{4\sigma_s}{3k_e}\frac{\partial T^4}{\partial y} \text{ (Rosseland approximation)}$$

Using $T^4 \cong 4T_m^3 T - 3T_m^4$ (Taylor series expansion about T_m) in above expression we get

$\frac{\partial q_r}{\partial y} = -\frac{16\sigma_s T_m^{\ 3}}{3k_e}\frac{\partial^2 T}{\partial y^2}$, so, equation (6) can be rewritten as

$$\rho C_p\left(\frac{\partial T}{\partial t} + u\frac{\partial T}{\partial x} + v\frac{\partial T}{\partial y}\right) = \left(\kappa + \frac{16\sigma_s T_m^{\ 3}}{3k_e}\right)\frac{\partial^2 T}{\partial y^2} + \mu\left(\frac{\partial u}{\partial y}\right)^2 + \sigma_e B^{*2}u^2 + Q^*\left(T - T_s\right), \quad (7)$$

Equation of concentration

$$\frac{\partial C}{\partial t} + u\frac{\partial C}{\partial x} + v\frac{\partial C}{\partial y} = D\frac{\partial^2 C}{\partial y^2} - k_1^*(C - C_s), \quad (8)$$

where D is mass diffusivity, $k_1^* = k_1\left(1-at\right)^{-1}$ is chemical reaction rate and C_s is concentration of fluid at stationary wall.

The boundary conditions [Siddiqui *et al.* (2008)] are

$$y = 0: \quad \frac{\partial u}{\partial y} = 0,\ v = 0,\ T = T_s,\ C = C_s;$$
$$y = h(t): u = 0, v = v_w\left(t\right), T = T_m, C = C_m. \quad (9)$$

3. METHOD OF SOLUTION

Introducing the following similarity variable, functions and dimensionless parameters:

$$u = \frac{a\,x}{(1-at)}\,f'(\eta), v = -\frac{a\,d}{(1-at)^{1/2}}\,f(\eta),$$
$$\eta = \frac{y}{d\,(1-at)^{1/2}}, \theta = \frac{T - T_s}{T_m - T_s}, \phi = \frac{C - C_s}{C_m - C_s}, \quad (10)$$

where η is the similarity variable, θ is the dimensionless temperature, ϕ is the dimensionless concentration, $f\left(\eta\right)$ is the dimensionless stream function and prime denotes the differentiation with respect to η. Now using equation (10) into the equations (5), (7) and (8) we have

$$f^{iv} - Sq(2\,f'f'' + \eta\,f''' - 2\,f\,f''' + 3\,f'') - \left(M + K\right)f'' = 0, \quad (11)$$

eISSN 1303-5150

$$\left(1+\frac{4}{3}Rd\right)\theta^{''}-Sq\,Pr\,(\eta\,\theta^{'}-2\,f\,\theta^{'}) + Pr\,Ec\,f^{''2}+Jh\,f^{'2}+Pr\,Q\,\theta=0, \quad (12)$$

$$\phi''-Sq\,Sc\left(\eta\,\phi'-2\,f\,\phi'+2k\phi\right)=0, \quad (13)$$

where $Sq\left(=\frac{a\,d^2}{2\nu}\right)$ is the dimensionless squeeze number which describes the movement of the plates, $M\left(=\frac{\sigma_e\,B_0^2\,d^2}{\rho\nu}\right)$ is the Magnetic parameter, $K\left(=\frac{d^2}{K_0}\right)$ is permeability parameter, $Rd\left(=\frac{4\sigma_s T_m^{\,3}}{\kappa\,k_e}\right)$ is the radiation parameter, $Pr\left(=\frac{\mu C_p}{\kappa}\right)$ is the Prandtl number, $Ec\left(=\frac{a^2\,x^2}{C_p\,(T_m-T_s)(1-at)^2}\right)$ is the Eckert number, $Jh\left(=Pr.Ec.M\right)$ is Joule heating parameter, $Q\left(=\frac{Q_0\,d^2}{\mu C_p}\right)$ is the dimensionless heat generation/absorption parameter, $Sc\left(=\frac{\nu}{D}\right)$ is the Schmidt number and $Cr\left(=\frac{k_1}{a}\right)$ is the chemical reaction parameter.

The boundary conditions in dimensionless form are reduced to

$$\eta=0:\ f=0,\ f''=0,\ \theta=0,\ \phi=0;$$
$$\eta=1:\ f=1/2,\ f'=0,\theta=1,\phi=1. \quad (14)$$

Skin friction Coefficient, Nusselt number and Sherwood number

Rate of shear stress in terms of skin friction coefficient at the lower stationary plate is given by

$$C_f=\frac{\tau_w}{\rho v_w^2}$$
$$\Rightarrow \frac{d^{\,2}(1-at)^{1/2}}{2\,x^2}\,Re_x\,C_f=\left[\,f''(\eta)\right]_{\eta=1}, \quad (15)$$

where τ_w is the wall shear stress given by $\tau_w=\mu\left(\frac{\partial u}{\partial y}\right)_{y=h(t)}$ and $Re_x\left(=\frac{a\,d\,x}{2\nu}\right)$ is the local squeeze Reynolds number.

Rate of heat transfer in terms of Nusselt number at the plates is given by

$$Nu=\frac{d\,q_w}{\kappa(T_m-T_s)}$$
$$\Rightarrow(1-at)^{1/2}\,Nu=-\left[\theta'(\eta)\,\right]_{\eta=0\&1}, \quad (16)$$

where q_w is the rate of heat transfer given by $q_w=-\kappa\left(\frac{\partial T}{\partial y}\right)_{y=0\&h(t)}$.

Rate of mass transfer in terms of Sherwood number at the plates is given by

$$Sh=\frac{d\,q_m}{D(C_m-C_s)}$$
$$\Rightarrow(1-at)^{1/2}\,Sh=-\left[\phi'(\eta)\,\right]_{\eta=0\&1}, \quad (17)$$

where q_m is the rate of mass transfer given by $q_m=-D\left(\frac{\partial C}{\partial y}\right)_{y=0\&h(t)}$.

Equation (11) is the nonlinear ordinary forth order differential equation and equation (12)-(13) are the coupled nonlinear ordinary second order differential equations. These equations along with boundary conditions (14) are solved numerically using fourth order Runge-Kutta method along with shooting technique on MATLAB software. First, we convert the boundary value problem into

eISSN 1303-5150

the initial value problem with systematic guessing of the values of $f'(0)$, $f'''(0)$, $\theta'(0)$ and $\phi'(0)$ by the shooting technique until the boundary conditions at $\eta = 1$ are satisfied and then solved by using fourth order Runge-Kutta method with step-size $h = 0.001$.

4. RESULTS AND DISCUSSION

The effects of different physical parameters on velocity, temperature and concentration distribution are discussed through figures. Effect of squeeze number on velocity distribution is displayed in figure 2. $Sq > 0$ corresponds to the movement of upper plate towards the lower static plate while $Sq < 0$ stands for its movement far away from the lower plate. It is depicted from figure 2 that fluid velocity decreases near the lower static plate as the squeeze number increases, while reverse behavior is observed as moves toward upper plate. The effect of Magnetic parameter on velocity of the fluid is displayed in figure 3. Due to magnetic field, a resisting force is generated in the flow which is called Lorentz force. This force caused a decline in velocity of the fluid near the lower plate, while opposite trend is observed near the upper plate. Same effects of squeeze number and Magnetic parameter on velocity profile are mentioned in Ahmed *et al.* (2015). In this problem we have considered that channel is filled with porous substance. The effect of porosity of medium is shown through figure 4. It is depicted that fluid velocity decreases near the lower plate as permeability parameter increases while reverse behavior is seen as moves toward upper plate.

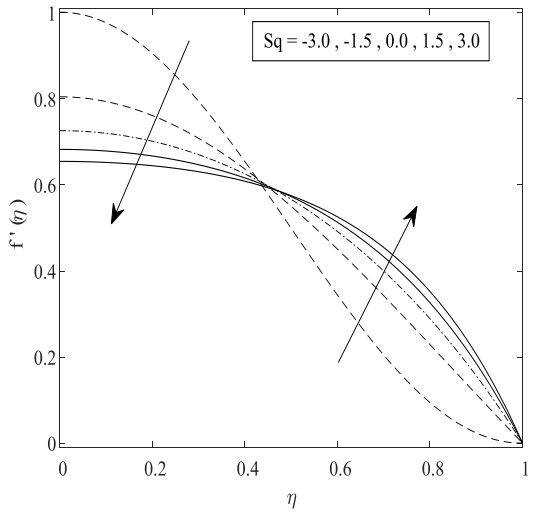

Fig.2. Velocity distribution with respect to Squeezing parameter.

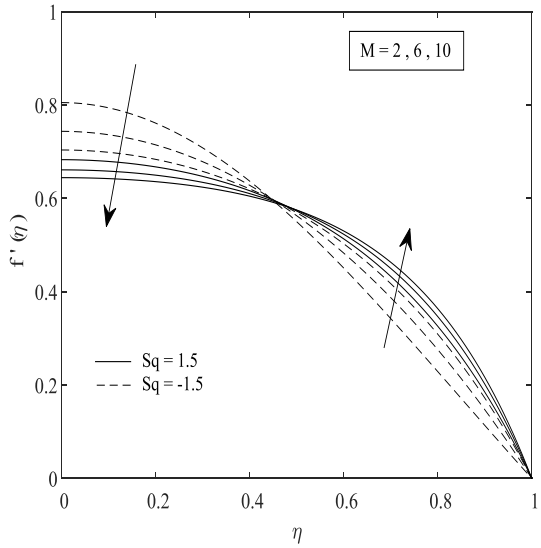

Fig.3. Velocity distribution with respect to Magnetic parameter.

It is observed from figure 5 that fluid temperature increases for increasing values of the squeeze number. This behavior is due to the fact that an increase in squeeze number represents the increase in the speed at which the upper plate moves towards lower plate. Consequently, the friction between the boundary surface of the plates and fluid increases and so the temperature of the fluid.

eISSN 1303-5150

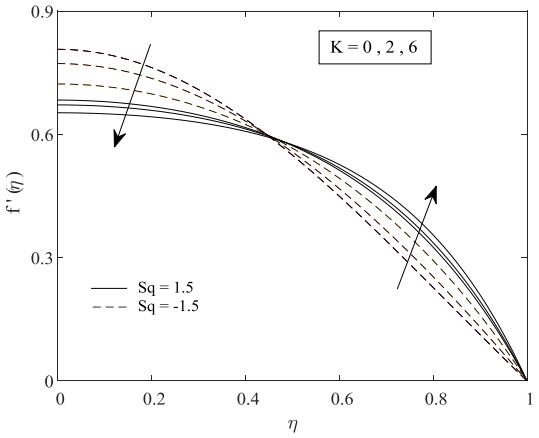

Fig.4. Velocity distribution with respect to permeability parameter.

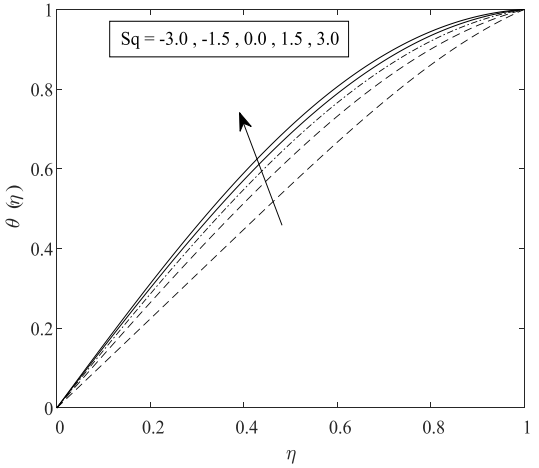

Fig.5. Temperature distribution with respect to Squeezing parameter.

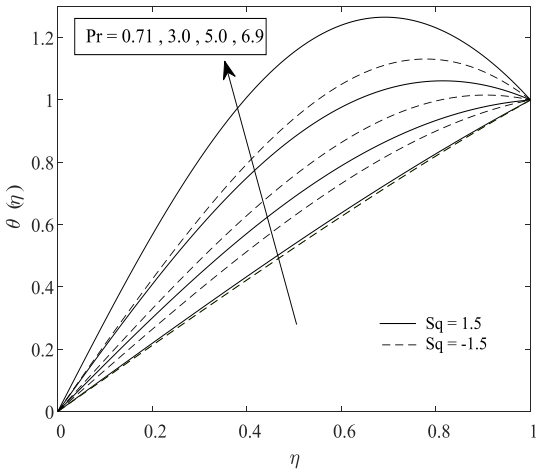

Fig.6. Temperature distribution with respect to Prandtl number.

It is seen from figure 6 that as the Prandtl number increases the temperature field also increases. Figure 7 shows the effects of Eckert number on temperature distribution and it declares that temperature field increases with the increase of Eckert number which is as a result of frictional heating. It is depicted from figure 8 that the temperature field increases as the heat generation/absorption parameter increases. Increment in heat generation parameter indicates that external heat is provided to fluid and clearly it causes the enhancement of the fluid temperature. Radiation parameter effect on temperature field is demonstrated by figure 9 and it is seen that temperature field is diminished with radiation parameter. Joule heating parameter's effect on temperature field is demonstrated in figure 10 and it is observed that temperature profiles are elevated with the increment of Joule heating parameter for both $Sq > 0$ and $Sq < 0$. Concentration profiles are shown in figures 11-13. Squeeze parameter's effect on concentration field is shown in figure 11. It is observed that with the increasing values of squeeze number concentration profiles gradually decline. Figure 12 illustrates the effect of Schmidt number on concentration profile and it is depicted that concentration profiles diminish with the increasing values of Schmidt number. From figure 13 it is clear that as we increase the chemical reaction parameter, the concentration profiles decrease.

eISSN 1303-5150

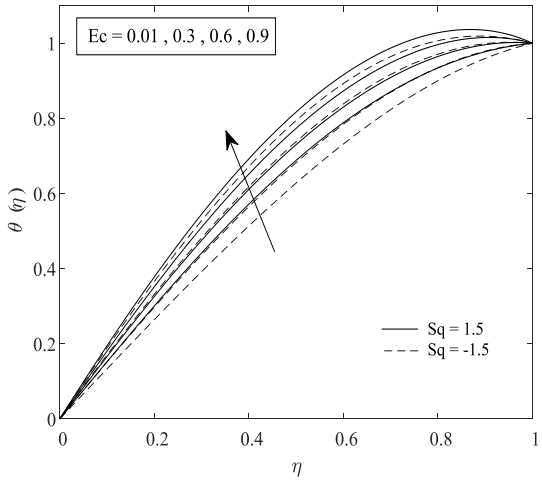

Fig.7. Temperature distribution with respect to Eckert number.

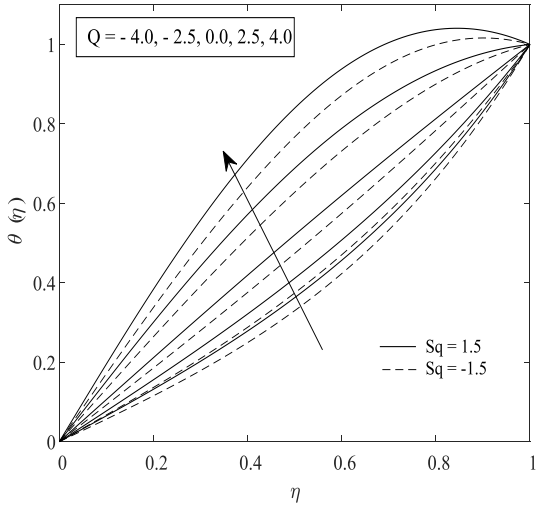

Fig.8. Temperature distribution with respect to Heat generation/absorbtion parameter.

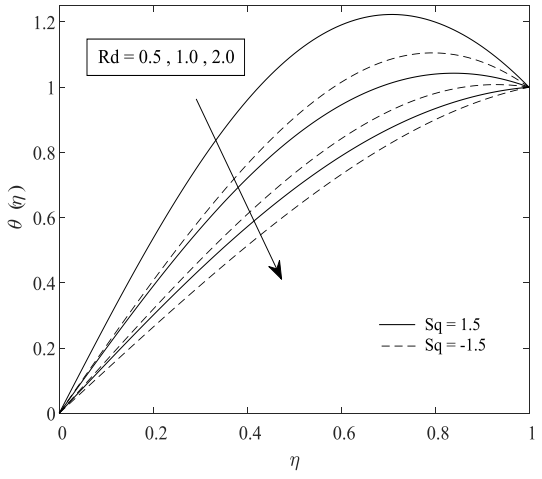

Fig.9. Temperature distribution with respect to radiation parameter.

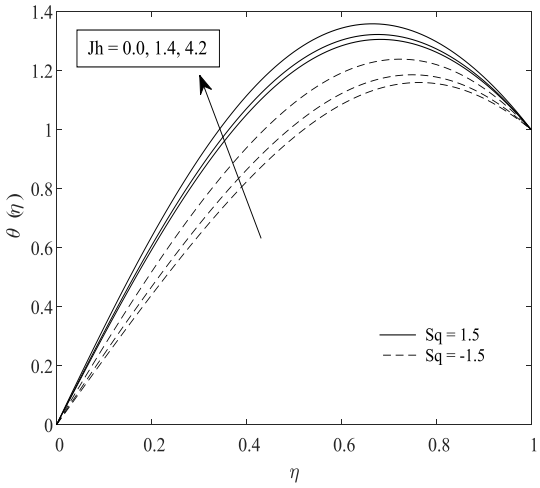

Fig.10. Temperature distribution with respect to Joule heating parameter.

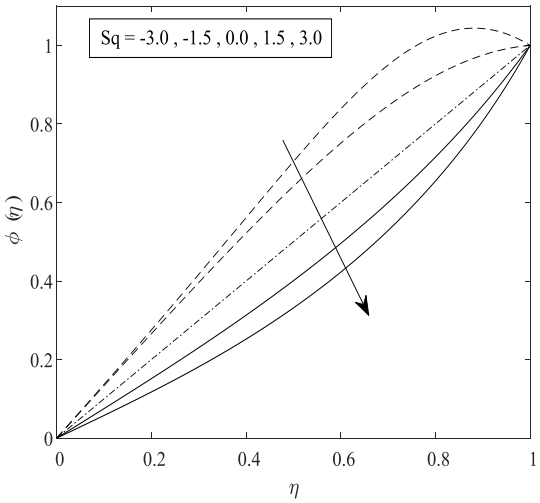

Fig. 11. Concentration distribution with respect to Squeezing parameter.

eISSN 1303-5150

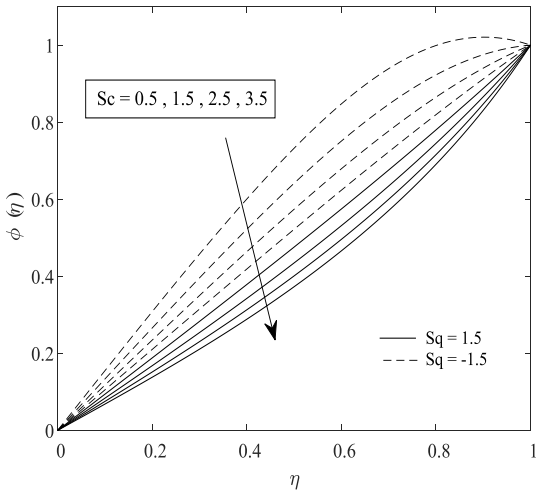

Fig. 12. Concentration distribution with respect to Schmidt number.

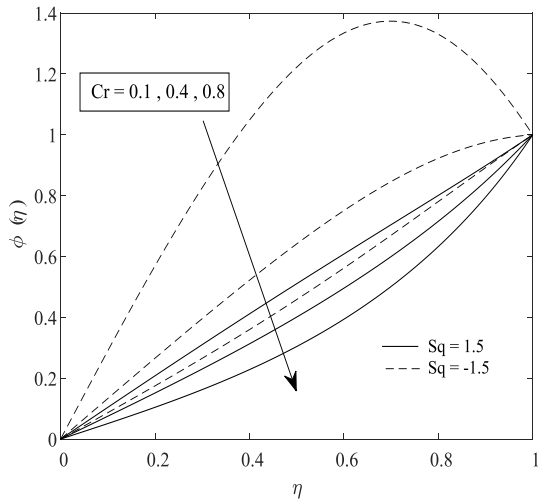

Fig. 13. Concentration distribution with respect to chemical reaction parameter.

Table 1: Numerical values of skin friction coefficient at upper plate.

M	K	$f''(1)$	
		$Sq=-1.5$	$Sq=1.5$
2.0	0.1	-1.118965	-2.110944
6.0		-1.574472	-2.376943
10.0		-1.932061	-2.614969
2.0	2.0	-1.351504	-2.241331
	6.0	-1.753427	-2.493018

Table 2: Numerical values of Nusselt number at lower and upper plates.

Rd	Jh	Pr	Ec	Q	$-\theta'(0)$		$-\theta'(1)$	
					$Sq=-1.5$	$Sq=1.5$	$Sq=-1.5$	$Sq=1.5$

eISSN 1303-5150

0.5	0.06	3.0	0.01	2.5	-1.333928	-1.529314	-0.302698	-0.122511
1.0					-1.618830	-2.002709	0.227878	0.532639
2.0					-2.076567	-2.784833	1.010272	1.478070
0.5	0.3				-1.379291	-1.528687	-0.267555	-0.123483
	0.6				-1.414175	-1.533446	-0.238931	-0.119842
	0.06	5.0			-1.676439	-2.100007	0.330322	0.6557841
		6.9			-2.170385	-2.946943	1.163398	1.660204
		3.0	0.3		-1.532048	-1.679224	-0.093726	0.108991
			0.6		-1.7369992	-1.834303	0.122452	0.348476
			0.01	0.0	-0.923760	-1.061124	-1.087989	-0.925773
				-2.5	-0.671038	-0.771668	-1.683159	-1.534588

Table 3: Numerical values of Sherwood number at lower and upper plates.

Sc	Cr	$-\phi'(0)$		$-\phi'(1)$	
		$Sq=-1.5$	$Sq=1.5$	$Sq=-1.5$	$Sq=1.5$
2.5	0.4	-1.335545	-0.749080	-0.100122	-1.662546
1.5		-1.175293	-0.833808	-0.511424	-1.423694
0.5		-1.051761	-0.938197	-0.850409	-1.151819
2.5	0.1	-0.865425	-1.043963	-1.052212	-1.045829
	0.8	-2.920072	-0.506312	2.371639	-2.317655

Tables 1-3 display the numerical values of the skin friction coefficient, Nusselt number and Sherwood number for different values of flow parameters. It is observed from Table 1 that the skin friction coefficient at the upper moving plate decreases with the increase of the Magnetic parameter for both $Sq>0$ and $Sq<0$. It is also noted from Table 1 that skin friction coefficient is a decreasing function of the squeeze number.

It is seen from Table 2 that the Nusselt number decreases at the lower plate with the increase of the squeeze number, while an opposite behavior is observed at the upper plate. The Joule heating parameter decreases the Nusselt number at lower plate for $Sq<0$, while at the upper plate, reverse behavior is observed. It is also depicted that due to increase of Prandtl number, Eckert number or heat source/sink parameter the Nusselt number decreases at the lower static plate; while it increases at the upper moving plate for both $Sq>0$ and $Sq<0$. With the radiation parameter Nusselt number shows different behavior. When the radiation parameter increases Nusselt number increases at the lower plate; while it decreases at the upper moving plate for both $Sq>0$ and $Sq<0$. Table 3 shows the effects of Schmidt number and chemical reaction parameter on Sherwood number. It is observed that for Schmidt number or chemical reaction parameter, the Sherwood number decreases at the lower plate when $Sq<0$ and increases when $Sq>0$, while at the upper plate, the Sherwood number

eISSN 1303-5150

decreases when $Sq > 0$ and it increases when $Sq < 0$.

5. CONCLUSIONS

The unsteady MHD flow, heat and mass transfer through an incompressible electrically conducting viscous fluid squeezed between two infinite non conducting parallel plates separated by variable distance is investigated. Governing transport equations are reduced to non-linear ordinary differential equations using some similarity transforms and solved by using Runge-Kutta fourth order method with shooting technique on MATLAB software. The effects of different physical parameters on fluid velocity, temperature, concentration, skin friction coefficient, Nusselt number and Sherwood number are discussed and the following observations are made:

1. As the Magnetic parameter or permeability parameter increases, the fluid velocity decreases near the lower static plate; whereas near the upper moving plate the fluid velocity increases.
2. The fluid temperature increases with the increase of heat generation/absorption parameter or Joule heating parameter; while it decreases with the radiation parameter.
3. The fluid concentration decreases as the squeeze number or Schmidt number or chemical reaction parameter increases.
4. The squeeze number decreases the skin friction coefficient, while it increases the Nusselt number at the upper moving plate.
5. The skin friction coefficient decreases while the Nusselt number at the upper plate increases as the Magnetic parameter increases.
6. The Sherwood number decreases at the lower plate when $Sq < 0$ and increases when $Sq > 0$ with Schmidt number or chemical reaction parameter, while at the upper plate behavior is opposite.

References

[1] Ahmed N, Khan U, Zaidi ZA, Jan SU, Waheed A and Mohyud-Din ST. MHD flow of an incompressible fluid through porous medium between dilating and squeezing permeable walls. J Porous Media 2014; 17(10): 861-867.

[2] Ahmed N, Khan U, Khan SI, Bano S and Mohyud-Din ST. Effects on magnetic field in squeezing flow of a Casson fluid between parallel plates, J of King Saud University Science 2015; DOI:10.1016/j.jksus.2015.03.006.

[3] Duwairi HM, Tashtoush B and Damseh RA. On heat transfer effects in a viscous fluid squeezed and extruded between two parallel plates. Heat Mass Transfer 2004; 41: 112-117.

[4] Hamza EA. The magneto hydrodynamic squeeze film. J Tribology 1988; 110: 375-377.

[5] Hayat T, Yousuf A, Mustafa M and Asghar S. Influence of heat transfer in the squeezing flow between parallel disks. Chem Eng Comm 2012; 199: 1044-1062.

[6] Jackson JD. A study of squeezing flow. Appl Sci Res A 1962; 11: 148-152.

[7] Jyothi AM, Kumar RSV, Madhukesh JK, Prasannakumara BC and Ramesh GK. Squeezing flow of Casson hybrid nanofluid between parallel plates with a heat source or sink and

eISSN 1303-5150

thermophoretic particle deposition. Heat Transfer 2021; 50(7): 7139-7156.

[8] Khan U, Ahmed N, Khan SIU, Zaidi ZA, Yang XJ and Mohyud-Din ST. On unsteady two-dimensional and axisymmetric squeezing flow between parallel plates. Alexandria Eng J 2014; 53: 463-468.

[9] Khan U, Ahmed N, Khan SIU, Bano S and Mohyud-Din ST. Unsteady squeezing flow of Casson fluid between parallel plates. World J Model Simul 2014; 10(4): 308-319.

[10] Mahmood M, Asghar S and Hossain MA. Squeezed flow and heat transfer over a porous surface for viscous fluid. Heat Mass Transfer 2007; 44: 165-173.

[11] Makinde OD, Motsumi TG, Ramollo MP. Squeezing flow between parallel plates: A bifurcation study. Far East Jour Appl Math 2002; 9(2): 81-94.

[12] Mustafa M, Hayat T and Obaidat S. On heat and mass transfer in the unsteady squeezing flow between parallel plates. Meccanica 2012; 47: 1581-1589.

[13] Qayyum M and Oscar I. Exploration of unsteady squeezing flow through Least Squares Homotopy Perturbation Method. Hindawi Journal of Mathematics 2021; Article ID 2977026, 12 pages DOI:10.1155/2021/2977026.

[14] Siddiqui M, Irum S and Ansari AR. Unsteady squeezing flow of a viscous MHD fluid between parallel plates, a solution using the Homotopy Perturbation Method. Mathematical Modelling and Analysis 2008; 13(4): 565-576.

[15] Sobamowo MG and Akinshilo AT. On the analysis of squeezing flow of nanofluid between two parallel plates under the influence of magnetic field. Alexandria Engineering Journal 2018; 57(3): 1413-1423.

[16] Sobamowo G, Jayesimi L, Oke D, Yinusa A and Adedibu O. Unsteady Casson nanofluid squeezing flow between two parallel plates embedded in a porous medium under the influence of magnetic field. Open J Math Sci 2019; 3: 59-73.

[17] Stefan MJ. Versuch Uber die scheinbare adhesion, Sitzungsberichte der Akademie der Wissenschaften in Wien. Mathematik-Naturwissen 1874; 69: 713-721.

[18] Wang CY. The squeezing of fluid between two plates. J Appl Mech 1976; 43(4): 579-583.

eISSN 1303-5150